DMD Fast Forward. Published on May 9, 2014 as doi: 10.1124/dmd.113.056309

Title Page

Hepatic uptake of atorvastatin: influence of variability in transporter expression on uptake clearance and drug-drug interactions

Anna Vildhede, Maria Karlgren, Elin K. Svedberg, Jacek R. Wisniewski, Yurong Lai, Agneta Norén, and Per Artursson

Department of Pharmacy, Uppsala University, Sweden (A.V, M.K, E.K.S, P.A); Uppsala University Drug Optimization and Pharmaceutical Profiling Platform (UDOPP) - a node of the Chemical Biology Consortium Sweden (M.K, P.A); Department of Proteomics and Signal Transduction, Max Planck Institute of Biochemistry, Martinsried D 82152, Germany (J.R.W); Pharmacokinetics, Dynamics and Drug Metabolism, Pfizer Global Research and Development, Pfizer Inc., Groton, Connecticut 06340, USA (Y.L); and Department of Surgery, Uppsala University, 751 85 Uppsala, Sweden (A.N)

Primary laboratory of origin: Department of Pharmacy, Uppsala University, Sweden

Running Title Page

Running title: Inter-individual variability in hepatic atorvastatin uptake

Corresponding author:

Per Artursson, PhD, Professor in Dosage Form Design

Department of Pharmacy, Uppsala University, Box 580, SE-751 23 Uppsala, Sweden

Phone: +46 – 18 471 44 71

Fax: +46 – 18 471 42 23

Email: per.artursson@farmaci.uu.se

Number of text pages: 36

Number of tables: 4

Number of figures: 7

Number of references: 41

Number of words in Abstract: 240

Number of words in Introduction: 307

Number of words in Discussion: 1520

Non-standard abbreviations:

AUC area under the plasma concentration-time curve

CL_{upt} uptake clearance

CYP cytochrome P450

DDI drug-drug interaction

DMEM Dulbecco's modified eagle medium

DPBS Dulbecco's phosphate buffered saline

HBSS Hank's balanced salt solution

IC_{50} half-maximal inhibitory concentration

KHB Krebs-Henseleit bicarbonate

K_m Michaelis-Menten constant

MTA maximal transport activity

NTCP sodium taurocholate co-transporting polypeptide

OATP organic anion transporting polypeptide

ORF open reading frame

SLC solute carrier

UPLC-MS/MS ultra-high performance liquid chromatography tandem mass spectrometry

V_{max} maximal uptake rate

DMD Fast Forward. Published on May 5, 2014 as DOI: 10.1124/dmd.113.056309

Abstract

Differences in the expression and function of the organic anion transporting polypeptide (OATP) transporters contribute to inter-individual variability in atorvastatin clearance. However, the importance of the bile acid transporter NTCP (*SLC10A1*) in atorvastatin uptake clearance (CL_{upt}) is not yet clarified. To elucidate this issue, we investigated the relative contribution of NTCP, OATP1B1, OATP1B3, and OATP2B1 to atorvastatin CL_{upt} in twelve human liver samples. The impact of inhibition on atorvastatin CL_{upt} was also studied, using inhibitors of different isoform specificities. Expression levels of the four transport proteins were quantified by LC-MS/MS. These data, together with atorvastatin *in vitro* kinetics, were used to predict the maximal transport activity (MTA) and inter-individual differences in CL_{upt} of each transporter *in vivo.* Subsequently, hepatic uptake impairment upon co-administration of five clinically interacting drugs was predicted using *in vitro* inhibitory potencies. NTCP and OATP protein expression varied 3.7- to 32-fold among the twelve sample donors. The rank order in expression was OATP1B1 > OATP1B3 ≈ NTCP ≈ OATP2B1. NTCP was found to be of minor importance in atorvastatin disposition. Instead, OATP1B1 and OATP1B3 were confirmed as the major atorvastatin uptake transporters. The average contribution to atorvastatin uptake was OATP1B1 > OATP1B3 >> OATP2B1 > NTCP, although this rank order varied between individuals. The inter-individual differences in transporter expression and CL_{upt} resulted in marked differences in drug-drug interactions due to isoform-specific inhibition. We conclude that this variation should be considered in *in vitro* to *in vivo* extrapolations.

Introduction

Transporter-mediated hepatic uptake of atorvastatin is the rate-determining step in the elimination of the drug *in vitro* (Watanabe *et al.*, 2010) and *in vivo* (Maeda *et al.*, 2011). At least four members of the SLC superfamily transport atorvastatin in various *in vitro* systems. These are the three organic anion transporting polypeptide transporters, OATP1B1 (*SLCO1B1*), OATP1B3 (*SLCO1B3*), and OATP2B1 (*SLCO2B1*) (Choi *et al.*, 2011; Karlgren *et al.*, 2012b; Konig, 2011), and the sodium taurocholate co-transporting polypeptide (NTCP, *SLC10A1*) (Choi *et al.*, 2011). All four proteins are expressed in the basolateral membrane of human hepatocytes, where they mediate uptake of substrates into the hepatocytes from the blood (Cui *et al.*, 2003; Keitel *et al.*, 2005).

The importance of OATP1B1 in the hepatic uptake has been emphasized, since OATP1B1 genetic variants with reduced function and OATP inhibition have been associated with greater systemic exposure of atorvastatin in clinical studies (Lau *et al.*, 2007; Pasanen *et al.*, 2007). However, in a recent study, NTCP was shown to contribute significantly to the hepatic uptake of three different statins (pitavastatin, fluvastatin, and rosuvastatin) with 24-45 % of overall active uptake (Bi *et al.*, 2013). These results indicate that NTCP may play a more important role in statin uptake than previously assumed. The importance of NTCP in atorvastatin uptake has not yet been clarified and needs to be addressed.

In the present study, we investigated the contribution of NTCP to hepatic atorvastatin uptake using a protein expression based prediction model (Karlgren *et al.*, 2012b) and *in vitro* hepatocyte experiments. We combined *in vitro* uptake kinetics with protein quantification to assess the contribution of each transporter to atorvastatin uptake clearance (CL_{upt}) in livers from twelve individuals with varying expression of the four uptake transporters. We also investigated the influence of inter-individual transporter expression and isoform-specific inhibition on atorvastatin clearance at clinically relevant concentrations.

Materials and Methods

Compounds

Atorvastatin was kindly provided by AstraZeneca (Mölndal, Sweden). Atazanavir was acquired from Toronto Research Chemicals Inc. (Toronto, ON, Canada). Cyclosporine, gemfibrozil and rifampicin were purchased from Sigma-Aldrich (St. Louis, MO, USA), and lopinavir from Abbott Laboratories (Chicago, IL, USA). All other chemicals were of analytical grade and purchased from commercial sources.

Cloning and establishment of stable NTCP-HEK293 cells

Total human liver RNA was obtained from Clontech (Mountain View, CA, USA). cDNA was generated by reverse transcription using the SuperScript III first-strand synthesis supermix (Invitrogen, Carlsbad, CA, USA). A NTCP-pcDNA5/FRT vector was constructed in two steps. First, the NTCP open reading frame (ORF) was amplified from the human liver cDNA using Platinum *Pfx* DNA polymerase (Invitrogen, Carlsbad, CA, USA) and the gene-specific primer pair 5'-CTAGAAGCTTATGGAGGCCCACAACGCGTC-3'/5'-CTAGGGTACCGGGGCTGTGCAAGGGGAGCAGT-3'. Restriction sites introduced by the primers are underlined. The PCR product was cloned into the *Hind*III/*Kpn*I site of the vector p3xFLAG-CMV14 (Sigma-Aldrich, St. Louis, MO, USA). The inserted NTCP ORF was verified by DNA sequencing analysis and found to be identical to the NCBI *SLC10A1* reference sequence (NM_003049).

Next, the NTCP-p3xFLAG-CMV14 was used as template in a second amplification step with Platinum *Pfx* DNA polymerase (Invitrogen, Carlsbad, CA, USA) and the primer pair 5'-CTAGAAGCTTATGGAGGCCCACAACGCGTC-3'/5'-CTAGCTCGAGCTACTTGTCATCGT CATCCT-3'. *Hind*III and *Xho*I restriction sites introduced by the primers are underlined. The PRC product, consisting of the NTCP ORF with a FLAG-tag, was cloned into the *Hind*III/*Xho*I site of the expression vector

pcDNA5/FRT (Invitrogen, Carlsbad, CA, USA). The inserted sequence was verified by DNA sequencing analysis. Human embryonic kidney (HEK) Flp-In-293 cells (Invitrogen, Carlsbad, CA, USA) were transfected with the constructed NTCP-pcDNA5/FRT expression vector and further selected using hygromycin B (Invitrogen, Carlsbad, CA, USA) as previously described (Karlgren *et al.*, 2012a).

Cell cultivation

Mock-transfected HEK Flp-In-293 cells and cells stably expressing NTCP or either of the three OATP transporters (established and characterized by (Karlgren *et al.*, 2012a; Karlgren *et al.*, 2012b)) were cultivated as described elsewhere (Karlgren *et al.*, 2012a). Passages between 10 and 30 were used throughout the study.

Transport experiments in HEK293 cells

Two days before transport experiments, OATP2B1-expressing cells were seeded in 96-well CellBind plates (Corning, Amsterdam, Netherlands) at a density of 100,000 cells per well. Cells expressing NTCP, OATP1B1, or OATP1B3 were seeded in 24-well plates at a density of 600,000 cells per well two (OATP1B1, NTCP) or three days (OATP1B3) before the experiments. For all cultures in 96- or 24-well plates, Flp-In medium without phenol red and hygromycin B was used. Cell density was optimized by a computer assisted experimental design (MODDE 7.0, Umetrics, Umeå, Sweden) (Karlgren *et al.*, 2012a).

The following experimental procedure was used in both the kinetic and inhibition experiments. At start of the experiment, cells were washed twice with pre-warmed Hank's balanced salt solution (HBSS), pH 7.4, followed by incubation with pre-warmed substrate or substrate/inhibitor solutions for 2 min at 37 °C. The incubation was terminated by adding ice-cold Dulbecco's phosphate buffered saline (DPBS), followed by two-three washes with ice-cold DPBS. The cells were dried and the intracellular drug accumulation was quantified by ultra-high performance liquid chromatography-tandem mass spectrometry (UPLC-MS/MS).

All transport experiments in HEK293 cells were run in duplicate (24-well format) or triplicate (96-well format) on at least two independent separate occasions.

Kinetic characterization of NTCP- and OATP-mediated atorvastatin uptake

The uptake of atorvastatin in HEK293 cells stably expressing NTCP was linear up to 6 min in the concentration range of 0.1-800 µM (data not shown). To assess the kinetics of the NTCP-mediated uptake of atorvastatin, we incubated NTCP-HEK293 cells for 2 min with increasing concentration of atorvastatin (0.1-500 µM). Initial uptake rate was plotted against substrate concentration. The resulting uptake curve was fitted to the Michaelis-Menten equation with the addition of a non-saturable passive diffusion rate component (Equation 1) using GraphPad Prism v.5.04 (GraphPad Software, La Jolla, CA, USA).

$$V = \frac{V_{max} \times [S]}{K_m + [S]} + P_{diff} \times [S] \qquad \text{Eq. 1}$$

where V is the uptake rate, V_{max} is the maximal uptake rate (at saturating substrate concentration), [S] is the substrate concentration, K_m is the substrate concentration at which the uptake rate is half of V_{max} and P_{diff} is the passive diffusion.

The Michaelis Menten kinetics of OATP1B1-, OATP1B3-, and OATP2B1-mediated uptake of atorvastatin have been previously determined (Karlgren *et al.*, 2012a; Karlgren *et al.*, 2012b). K_m and V_{max} data were used from these studies.

Concentration-dependent inhibition of NTCP- and OATP-mediated atorvastatin uptake

The half-maximal inhibitory concentrations, IC_{50}-values, of atazanavir, cyclosporine, gemfibrozil, lopinavir, and rifampicin for NTCP-, OATP1B1-, OATP1B3-, and OATP2B1-mediated atorvastatin uptake were determined *in vitro* using stably transfected HEK293 cells overexpressing each of the transporters. The inhibitors were selected to cover three well-known clinically interacting drugs causing *in vivo* atorvastatin AUC changes to varying extent

(cyclosporine, gemfibrozil, and rifampicin). In addition, two drugs (atazanavir and lopinavir) that interact clinically with other statins were included.

Substrate concentration was set to 1 µM and uptake was measured at seven to twelve inhibitor concentrations: 0.01-40 µM (atazanavir), 0.01-25 µM (cyclosporine), 0.01-1000 µM (gemfibrozil), 0.01-10 µM (lopinavir), and 0.01-630 µM (rifampicin). Cells incubated with 1 µM atorvastatin were used as a reference in the calculations of the remaining active uptake in the presence of the compound of interest. In all experiments, uptake in mock-transfected cells was subtracted from the total uptake to correct for the passive permeability. The resulting inhibition data were fitted to Equation 2 using GraphPad Prism v.5.04 (GraphPad Software, La Jolla, CA, USA) to estimate an IC_{50}-value.

$$\text{Substrate uptake (\% of control)} = \frac{100}{1+10^{\left(\text{Log}[\text{I}] - \text{Log}\text{IC}_{50}\right)\times Hillslope}} \qquad \text{Eq. 2}$$

where [I] is the inhibitor concentration and the Hill slope describes the steepness of the curve. The equation is equal to the four-parameter equation when the top plateau of the curve is constrained to 100 % and the bottom plateau is fixed to 0 % in the data fitting.

As previously defined, a compound was considered to be a specific inhibitor of a transporter if the IC_{50}-value was at least 10-fold lower than the IC_{50}-values of the other three transporters (Karlgren *et al.*, 2012b). On the basis of the IC_{50}-values, corresponding inhibition constants, K_i, were calculated assuming competitive inhibition (Equation 3).

$$K_i = \text{IC}_{50} \,/\, \left(\frac{[\text{S}]}{K_m} + 1 \right) \qquad \text{Eq. 3}$$

UPLC-MS/MS analysis

Intracellular atorvastatin was extracted with 200 µl acetonitrile/water (60/40) spiked with 50 nM warfarin as internal standard, followed by centrifugation at 2465 x *g* at 4 °C for 20 min. Atorvastatin concentration in the supernatant was determined using UPLC-MS/MS

with the following analytical system: Acquity UPLC with a reversed phase BEH C18 column (2.1 x 50 mm, particle size 1.7 µm) (Waters, Milford, MA, USA) and a mobile gradient consisting of acetonitrile, formic acid and water, coupled to a Waters Xevo triple quadrupole with electrospray ionization interface.

Protein concentration

In all uptake kinetic or inhibition experiments, total protein content was measured in representative wells using the BCA Protein Assay Reagent Kit (Pierce Biotechnology, Rockford, IL, USA).

Human liver tissue

Normal excess human liver tissue was obtained from liver resections carried out at the Department of Surgery, Uppsala University Hospital (Uppsala, Sweden), as approved by Uppsala Regional Ethical Review Board (ethical approval no. 2009/028). All donors gave their informed consent. Twelve snap-frozen liver biopsy samples were used for analysis of hepatic protein expression. Another five human liver tissue specimens were used for hepatocyte isolation and subsequent uptake experiments. A summary of donor characteristics can be found in Supplemental Table 1. All donors were of Caucasian origin. The donors had no history of HIV or hepatitis.

Transport experiments in human hepatocytes

Primary hepatocytes were isolated using a two-step collagenase perfusion technique described elsewhere (Lecluyse *et al.*, 2010). The cells were suspended in DMEM supplemented with 5 % FBS, penicillin-streptomycin (PEST,100 U ml^{-1} and 100 µg ml^{-1}, respectively), 4 µg ml^{-1} insulin and 1 µM dexamethasone, and plated on collagen I-coated 24-well plates (BD Biosciences, Franklin Lakes, NJ, USA) at a density of 375,000 cells per well. The cells were allowed to attach for 3 h at 37 °C and 5 % CO_2 atmosphere. After attachment, the medium was replaced with Hepatocyte Maintenance Medium (Lonza, Basel, Switzerland)

supplemented with PEST, insulin-transferrin-selenium (10 µg ml^{-1}, 5.5 µg ml^{-1}, and 5 ng ml^{-1}, respectively) and 0.1 µM dexamethasone.

NTCP-mediated uptake of atorvastatin

Twenty-four hours post-seeding, the cells were washed twice with either pre-warmed modified Krebs-Henseleit bicarbonate (KHB) buffer (1.2 mM $MgSO_4$, 0.96 mM KH_2PO_4, 4.83 mM KCl, 118 mM NaCl, 1.53 mM $CaCl_2$, 23.8 mM $NaHCO_3$, 12.5 mM HEPES, 5 mM glucose, pH 7.4) or sodium-free KHB (NaCl and $NaCHO_3$ replaced with choline chloride and $KHCO_3$ respectively, pH 7.4). This was followed by a pre-incubation with the sodium-containing/sodium-free KHB for 10 min at 37 °C. Pre-incubation medium was removed and drug transport was initiated by adding either atorvastatin (1 µM) or taurocholate (1 µM) in KHB or sodium-free KHB. Substrate concentration was selected to be in the vicinity of transporter Km (linear range) without violating the limit of detection in the mass spectrometric analysis. Uptake was terminated after 2 min by adding ice-cold DPBS. Cells were washed three times with DPBS and then dried. Intracellular accumulation of atorvastatin and taurocholate was determined with UPLC-MS/MS as described above. The experiment was run in quadruplicate on two separate occasions using hepatocytes isolated from two different donors.

Inhibition of atorvastatin uptake

At start of the experiment, cells were washed twice with pre-warmed HBSS, pH 7.4, followed by incubation with pre-warmed substrate or substrate/inhibitor solutions for 0.5, 1, 1.5 or 2 min at 37 °C. Atorvastatin concentration was set to 1 µM for reasons explained above. Since the hepatocyte experiments required a higher substrate concentration than that reached *in vivo* (due to sensitivity limitations in the mass spectrometric analysis), inhibitor concentration was scaled up to three times the predicted unbound inlet concentration to the liver in order to give a similar extent of uptake inhibition as in our *in vivo* predictions. Uptake

was terminated at designated time points by adding ice-cold DPBS, followed by three washes. Acetonitrile was added to stop atorvastatin metabolism and was then let to evaporate. Intracellular drug accumulation was quantified by UPLC-MS/MS as described above. Atorvastatin uptake was plotted against incubation time and initial uptake rate in absence and presence of inhibitor was determined from the slope of the curves. The experiment was run in triplicate on three separate occasions using hepatocytes isolated from two different donors and one in-house batch of cryopreserved hepatocytes from a third donor.

Quantitative protein expression analysis

Targeted protein quantification of NTCP in human liver and in NTCP-HEK293 cells

HEK293 cells stably transfected with NTCP were harvested and frozen down as previously described for HEK-OATP cells (Karlgren *et al.*, 2012b). Membrane fractions from the pellet of HEK293 cells were extracted and digested with trypsin using the protocol by Qui and colleagues (Qiu *et al.*, 2013). The plasma membrane constituted approximately 10% of the crude membrane fraction analyzed. The abundance of NTCP in HEK293 cells stably expressing the transporter relative to that in a representative human liver sample (previously prepared and analyzed for OATP1B1, OATP1B3 and OATP2B1 protein expression (Karlgren *et al.*, 2012b)) was determined by peptide-based LC-MS/MS measurements. An isotope-labeled peptide, unique for NTCP, was used as an internal standard to quantify the corresponding surrogate peptide of NTCP protein in both the cell line and human liver sample. Each sample was analyzed in duplicate (technical repeats).

Quantitative proteomic analysis of inter-individual differences in protein expression in the human liver samples

The protein expression levels of NTCP, OATP1B1, OATP1B3, and OATP2B1 in twelve human liver samples was determined from previously obtained in-depth label-free mass

spectrometry data (Karlgren *et al.*, 2012b) using the total protein approach (TPA) as described by (Wisniewski *et al.*, 2012).

In vitro to in vivo extrapolations

Prediction of hepatic intrinsic uptake clearance from protein expression levels

Hepatic intrinsic uptake clearance ($CL_{int,\ uptake}$) of atorvastatin was predicted from the maximal transport activity (MTA), calculated according to Equation 4 (Karlgren *et al.*, 2012b). Briefly, the ratio of the protein expression in a representative human liver sample to that in the overexpressing cell line (obtained using targeted peptide-based protein quantification) was used as a scaling factor to convert the maximal transport rate observed *in vitro* to a theoretical maximal transport activity *in vivo* (see Equation 5).

$$CL_{int,uptake} = \sum_{transporters} \frac{MTA}{K_m + [S]} \times HomPPGL \qquad \text{Eq. 4}$$

where [S] is the maximal unbound plasma concentration of atorvastatin and HomPPGL is milligrams of homogenate protein per gram of liver tissue.

$$MTA = \frac{Proteinexpression_{in\ vivo}}{Proteinexpression_{in\ vitro}} \times V_{max\ (in\ vitro)} \qquad \text{Eq. 5}$$

Using previously determined MTA values for atorvastatin transport by OATP1B1, OATP1B3, and OATP2B1 (Karlgren *et al.*, 2012b), and the MTA value obtained herein for NTCP, we predicted the intrinsic uptake clearance in the reference liver tissue sample. Uptake clearance for each of the twelve individuals was then predicted from the relative protein expression between different individuals, using the representative liver sample as reference.

Prediction of drug-drug interactions

In vitro inhibition data (K_i), were used to predict the impact of inhibition on atorvastatin intrinsic uptake clearance according to Equation 6 (Karlgren *et al.*, 2012b).

$$CL_{int,+inhibitor} = \sum_{transporters} \frac{CL_{int,uptake}}{\frac{[I]}{K_i} + 1} \qquad \text{Eq. 6}$$

The inhibitor concentration [I] in the predictions was the estimated maximal unbound concentration of the inhibitor at the inlet to the liver ($I_{u,max,in}$), as reported by (Yoshida *et al.*, 2012).

Data presentation and statistical analysis

Data are expressed as means ± standard deviations, unless otherwise stated. Differences in hepatic uptake in the presence and absence of sodium were assessed using Student's t-test. Results were deemed significant at $P < 0.05$.

DMD Fast Forward. Published on May 5, 2014 as DOI: 10.1124/dmd.113.056309

Results

Atorvastatin uptake in NTCP- and OATP-HEK293 cells

Atorvastatin uptake was 8-fold higher in cells expressing NTCP compared to mock-transfected cells (Figure 1A). The uptake followed Michaelis-Menten kinetics (Figure 1B). The K_m was determined to 185 ± 108 µM and V_{max} to 2260 ± 1184 pmol min^{-1} mg $protein^{-1}$, respectively (Table 1). OATP1B1-, OATP1B3-, and OATP2B1-mediated atorvastatin uptake kinetics have been determined previously (Karlgren *et al.*, 2012b) and are given in Table 1.

Inter-individual variability in protein expression of OATP1B1, OATP1B3, OATP2B1, and NTCP in human liver samples

Twelve human liver tissue samples were analyzed for expression of NTCP, OATP1B1, OATP1B3, and OATP2B1 using label-free mass spectrometry. The four transport proteins were detected in all twelve samples. The rank order in expression was OATP1B1 > OATP1B3 ≈ NTCP ≈ OATP2B1 (Figure 2A-D and Table 2). All of the uptake transporters displayed considerable variability in protein expression between the twelve individulas, ranging from 3.7-fold (OATP1B1) to 32-fold (OATP1B3), Table 2. However, the summed expression of the four transporters in the twelve livers only varied 2.3-fold.

Predictions of the intrinsic uptake clearance and contribution of NTCP, OATP1B1, OATP1B3, and OATP2B1 to atorvastatin uptake in vivo

The contribution of NTCP, OATP1B1, OATP1B3, and OATP2B1 to atorvastatin uptake *in vivo* (Figure 3) was predicted from atorvastatin uptake kinetics (Table 3) by correcting for the difference in membrane protein expression between the cell lines and the human liver samples. NTCP was predicted to play a minor role in the uptake with 1.5 to 10 % of total transporter-mediated uptake. Instead, OATP1B1 and OATP1B3 were confirmed to be the major uptake transporters with relative contributions of 26 to 89 and 1.8 to 60 % to the total

active uptake, respectively. In three of the twelve individuals (subject 5, 6 and 9), OATP1B3 was the primary transporter responsible for atorvastatin uptake into the liver. In contrast, the third hepatic OATP transporter, OATP2B1, generally played a less important role in the uptake with 3.2-30 % of total active uptake, (Figure 3). The rank order in average contribution was OATP1B1 > OATP1B3 >> OATP2B1 > NTCP.

For the twelve livers studied, a mean atorvastatin intrinsic uptake clearance of 2030 mL min^{-1} was predicted (95 % CI 1440-2620 mL min^{-1}). Assuming the same passive diffusion of atorvastatin across the cell membrane of hepatocytes and HEK293 cells, transporter-mediated active uptake was predicted to dominate with 90 ± 2 % (85-93 %) of overall atorvastatin uptake.

NTCP-mediated uptake of atorvastatin in human hepatocytes

NTCP has been shown to play a more significant role in the uptake of pitavastatin, fluvastatin, and rosuvastatin than what we predicted for atorvastatin. We therefore further investigated the validity of our predictions by studies in human hepatocytes. In this model, the sodium independent OATP transporters are active in parallel with the sodium-dependent NTCP. Hence, removal of sodium ions would incapacitate the NTCP transporter, but not the OATP transporters.

No significant difference in atorvastatin uptake in sodium-containing as compared to sodium-free buffer was observed, while the uptake of the prototypical NTCP substrate taurocholate was reduced by more than 50 % after removal of sodium, Figure 4 ($P < 0.001$). This result is consistent with our predictions of a low contribution of NTCP to hepatic atorvastatin accumulation.

Inhibition of NTCP- and OATP-mediated atorvastatin uptake in vitro

The dose-dependent inhibition of NTCP-, OATP1B1-, OATP1B3-, and OATP2B1-mediated atorvastatin uptake in HEK293 cells with atazanavir, cyclosporine, gemfibrozil,

lopinavir, and rifampicin is presented in Figure 5A-E. These drugs inhibit plasma clearance of atorvastatin or other statins in clinical DDI studies. The corresponding IC_{50}-values are summarized in Table 3. We defined an inhibitor as selective if the IC_{50}-value was at least 10 times lower than those of the other three transporters. On the basis of this definition, atazanavir, lopinavir and rifampicin were defined as selective OATP1B1 inhibitors for atorvastatin uptake (Figure 5A, D, and E). On the other hand, OATP2B1- and NTCP-mediated atorvastatin uptake was stimulated by rifampicin in a dose-dependent manner (Figure 5E). All of the uptake transporters, except for OATP2B1, were strongly inhibited by cyclosporine (Figure 5B). In contrast, gemfibrozil only interacted weakly with OATP1B1-, OATP2B1-, and NTCP-mediated transport of atorvastatin (IC_{50} > 50 μM), Figure 5C.

Predictions of the influence of DDIs on atorvastatin uptake clearance

The influence of co-administration of atazanavir, cyclosporine, gemfibrozil, lopinavir, or rifampicin on hepatic atorvastatin uptake clearance at clinically relevant concentrations was predicted for each human liver sample (Figure 6). In these predictions, the maximal unbound inlet concentration to the liver was used as inhibitor concentration, while maximal unbound plasma concentration was used for atorvastatin. Due to the variability in protein expression and isoform-specific inhibition (see above), marked differences in inhibition patterns were observed. For instance, co-administration of cyclosporine (an inhibitor of NTCP, OATP1B1, and OATP1B3) resulted in a low variability in inter-individual inhibition (40-57 % remaining active uptake clearance). In contrast, the OATP1B1 specific inhibitors atazanavir, lopinavir, and rifampicin showed greater variability between individuals with 20-57, 33-76, and 36-81 % remaining active uptake CL, respectively.

This can be explained by the isoform specificity of these compounds. While cyclosporine inhibits both OATP1B1 and OATP1B3 with similar potency, atazanavir, lopinavir, and rifampicin inhibit OATP1B1 with much higher potencies than OATP1B3. The summed

contribution of OATP1B1 and OATP1B3 to atorvastatin uptake CL showed lower inter-individual variability than the OATP1B1 contribution alone for these twelve livers. Hence, as illustrated here by atazanavir, lopinavir, and rifampicin, large differences in isoform-specific inhibitor potencies translate to high inter-individual variability in the inhibition of the hepatic atorvastatin uptake (Figure 6).

Overall, co-administration with atazanavir, an inhibitor with a relatively high estimated concentration at the inlet to the liver, was predicted to give the largest effect on atorvastatin uptake. Gemfibrozil, on the other hand, was predicted to have a minimal effect on atorvastatin uptake clearance due to its weak or non-existing inhibition of OATP1B1, OATP1B3, OATP2B1, and NTCP.

Inhibition of atorvastatin uptake in human hepatocytes

To verify our DDI predictions, we investigated the inhibition of the initial atorvastatin uptake in human hepatocytes from three donors (Figure 7). Two of the hepatocyte batches were used directly after isolation and one was a cryopreserved plateable batch from our collection of human hepatocytes. The uptake of atorvastatin was linear up to 2 min. The measured atorvastatin uptake clearance without inhibition was 5-12 µl min^{-1} mg $protein^{-1}$, which is similar to that measured independently in sandwich-cultured hepatocytes (unpublished data kindly provided by Dr. El-Kattan, Pfizer). In line with our predictions, cyclosporine was found to inhibit the uptake of atorvastatin by 44-74 % while gemfibrozil did not inhibit the uptake at all. Atazanavir inhibited the uptake by 26-45 %, i.e. in the lower range of our predictions. The other two inhibitors showed less inhibition than predicted from the liver tissue samples (lopinavir 0-30 %, and rifampicin 0-21 %).

Discussion

In a previous study, we introduced an expression based model to assess the contribution of each OATP to atorvastatin uptake clearance *in vivo* (Karlgren *et al.*, 2012b). Herein, we applied this model to study inter-individual differences in atorvastatin uptake clearance using liver tissue samples from twelve individuals. We also determined the contribution of NTCP to hepatic atorvastatin uptake for the first time.

NTCP and OATP protein levels were determined by label-free mass spectrometry. Our measured transporter abundances were comparable to previously reported hepatic expression data, albeit we find higher levels of OATP1B1 (Bi *et al.*, 2013; Kimoto *et al.*, 2012; Ohtsuki *et al.*, 2012; Prasad *et al.*, 2013). We speculate that this could be a result of the sample preparation used here (Wisniewski *et al.*, 2009), including the membrane fractionation, solubilization and tryptic digestion. The higher expression of OATP1B1 relative to NTCP, OATP1B3, and OATP2B1 confirms its importance in hepatic drug disposition.

Consistent with other reports (Nies *et al.*, 2013),we noted considerable inter-individual variability in transporter expression. The observed variability can be a result of e.g. differences in gene regulation, polymorphisms and/or epigenetic profiles (Ivanov *et al.*, 2012; Nies *et al.*, 2013) but it was outside the scope of this study to investigate this further.

Transporter abundances were used to determine the contribution of each transporter to atorvastatin uptake. Our method of predicting transporter contribution to uptake clearance builds on the assumptions that all protein quantified in the isolated membrane fraction is available to transport (Karlgren *et al.*, 2012b). Intracellular pools or post-translationally inactivated protein is not accounted for. Hence, the term maximal transport activity (MTA), which represents an upper limit in transport capacity. Although OATP transporters are reported not to be stored in intracellular vesicular compartments, NTCP has been shown to be subject to recycling from endosomal compartments (Roma *et al.*, 2008). It can thus not be

excluded that the abundance of NTCP in the cell membrane was overestimated. Nevertheless, this does not influence the interpretation of the results, since the contribution of NTCP to atorvastatin uptake was minor

Interestingly, the contribution of NTCP to atorvastatin uptake was much lower than previously reported for pitavastatin, fluvastatin and rosuvastatin (Bi *et al.*, 2013). Instead, we confirmed that OATP1B1 and OATP1B3 were the primary transporters involved in atorvastatin uptake *in vivo*. The importance of OATP1B1 in hepatic atorvastatin uptake has been emphasized in other studies (Amundsen *et al.*, 2010; Pasanen *et al.*, 2007), but our data suggest that OATP1B3 is almost as important. The relatively high contribution of OATP1B3 to the uptake of atorvastatin differs from other statins, such as simvastatin acid and pitavastatin (Elsby *et al.*, 2012; Hirano *et al.*, 2004). This observation is supported by a study on clinical pharmacokinetics of atorvastatin, in which OATP1B1 was predicted to account for 47 % of the total atorvastatin hepatic uptake (Shitara *et al.*, 2013). We attribute the remainder of the active uptake mainly to OATP1B3.

In contrast to OATP1B1 and OATP1B3, the third OATP transporter, OATP2B1, did not contribute substantially to hepatic uptake of atorvastatin. Instead, OATP2B1 may be important in the uptake of statins into skeletal muscle cells. OATP2B1 expression has been localized to the sarcolemmal membrane of human skeletal muscle fibers, suggesting that this protein has a key role in statin-related adverse effects in this tissue (Knauer *et al.*, 2010). OATP2B1 is also expressed in the human intestine and has been found to alter the AUC of drugs such as fexofenadine (Imanaga *et al.*, 2011). It may thus have an important role in intestinal absorption of statins.

Transporter-mediated drug-drug interactions were predicted for a set of clinical inhibitors with different isoform specificity using *in vitro* inhibitory data. Since OATP inhibition is substrate-dependent (e.g. (Noe *et al.*, 2007; Soars *et al.*, 2012)), the *in vitro* inhibitory

capacity was determined with atorvastatin as the victim drug. There were clear differences in OATP inhibition pattern when using atorvastatin as substrate instead of prototypical model substrates (Table 4). For instance, atazanavir, cyclosporine, and rifampicin showed a strong-to-moderate inhibition of OATP2B1-mediated uptake of estrone-3-sulphate, but no inhibition of atorvastatin transport. The substrate-dependent inhibition observed here and by others could be a result of multiple binding sites/domains on the OATP transporters (Miyagawa *et al.*, 2009; Noe *et al.*, 2007). We therefore recommend using substrates of concern, rather than model substrates, in *in vitro* studies aiming to predict *in vivo* interactions.

Atorvastatin uptake increased in the presence of rifampicin in a concentration-dependent manner in OATP2B1- and NTCP-expressing HEK293 cells. Since the contribution of these transporters to overall atorvastatin uptake was limited, this stimulation was not accounted for in our DDI predictions. Stimulation of OATP uptake has been reported previously in *in vitro* studies (Grube *et al.*, 2006). To our knowledge, though, it has never been observed *in vivo*. There is evidence of *in vivo* stimulation of efflux transport by the multidrug resistance associated protein 2 (MRP2) in rats (Heredi-Szabo *et al.*, 2009), but the degree of potentiation is much less than that observed *in vitro* in the same study.

Marked differences in the predicted extent of drug-drug interactions were observed between the individuals as a result of the variability in transporter contribution to atorvastatin uptake (Figure 6). This illustrates the importance of investigating the relative contribution of all transporters involved in the uptake of drug substrates in order to correctly assess the impact of drug-drug interactions of various isoform-specific inhibitors. Our MTA-based approach can easily be applied for this purpose and gives accurate predictions of transporter contribution without the need of either *in vivo* studies of reduced function genetic variants or human hepatocyte experiments with transporter-specific substrates (relative activity factor (RAF)) (Hirano *et al.*, 2004). It should be noted that the expression-based scaling factor is *in*

vitro system-specific and thus needs to be determined for each cell line used. Once it has been established though, it can be applied to any substrate.

In vitro experiments in human hepatocytes confirmed our DDI predictions. Although the hepatocytes were isolated from different tissue samples than those used for our predictions, the results were in good agreement. Lopinavir and rifampicin, though, gave less inhibition than predicted and the inhibition by atazanavir was in the lower range of our predictions. This could indicate that the hepatic OATP1B1 expression/availability was lower in these hepatocyte batches than in the human liver tissue samples (Kimoto *et al.*, 2012; Lundquist *et al.*, 2014).

The DDI predictions were included to illustrate the possible consequence of large inter-individual variability in transporter expression on the extent of impaired hepatic uptake, potentially translating to variability in systemic exposure. Our predictions agreed qualitatively with clinical observations. Gemfibrozil was predicted to have a low impact on atorvastatin uptake CL *in vivo*. The reported AUC changes upon concomitant administration of this drug with atorvastatin are also relatively small (1.2- to 1.4-fold) (Backman *et al.*, 2005; Whitfield *et al.*, 2011)). In contrast, cyclosporine and rifampicin were predicted to reduce the hepatic uptake by approximately 50 % and these compounds increase atorvastatin AUC to a large extent *in vivo* (>7-fold AUC change, (Asberg *et al.*, 2001; He *et al.*, 2009; Hermann *et al.*, 2004; Lau *et al.*, 2007; Lemahieu *et al.*, 2005)). Although hepatic uptake plays a major role in clinically observed drug-drug interactions with atorvastatin as the victim drug, inhibition of CYP3A4-mediated metabolism and efflux in both the intestine and liver is likely to contribute to the AUC changes seen *in vivo*. Gemfibrozil and rifampicin are CYP3A4 non-inhibitors (Maeda *et al.*, 2011; Wen *et al.*, 2001), but cyclosporine is a potent inhibitor of CYP3A4 and its pronounced effect on atorvastatin AUC may reflect this complexity.

DMD Fast Forward. Published on May 5, 2014 as DOI: 10.1124/dmd.113.056309

In conclusion, the present study showed that quantification of drug transport protein expression can advance our understanding of inter-individual differences in hepatic uptake and drug-drug interactions. We found substantial differences in the expression of NTCP, OATP1B1, OATP1B3, and OATP2B1 in twelve human liver samples. As a consequence, the contribution of these transporters to hepatic uptake influenced the potential for DDI with co-administered drugs at the individual level. We confirm a dominating role of OATP1B1 and OATP1B3 in the uptake clearance of atorvastatin, while NTCP and OATP2B1 play minor roles. Our study provides proof-of-concept that differences in transporter expression must be taken into account in predictions of variability in drug clearance and clinical drug-drug interactions for drugs that are substrates of several transporters.

Acknowledgements

The authors gratefully acknowledge Drs. Ulf Haglund, Frans Duraj and Jozef Urdzik at Uppsala University Hospital for their skillful contribution in clinical sampling. We are indebted to Drs. Xi Qiu and Emi Kimoto at Pfizer for their contribution to the protein quantification. Dr. Ewa Ellis at Karolinska Institutet is acknowledged for kindly providing one of the hepatocyte batches used in the DDI experiments. The authors also thank Cherendeep Dhanda for her valuable contribution in transport experiments.

Authorship Contributions

Participated in research design: Vildhede, Karlgren, Artursson

Conducted experiments: Vildhede, Karlgren, Svedberg, Wisniewski, Lai, Norén

Contributed new reagents or analytical tools: Wisniewski, Lai

Performed data analysis: Vildhede

Wrote or contributed to the writing of the manuscript: Vildhede, Karlgren, Svedberg, Wisniewski, Lai, Norén, Artursson

References

Amundsen R, Christensen H, Zabihyan B and Asberg A (2010). Cyclosporine A, but not tacrolimus, shows relevant inhibition of organic anion-transporting protein 1B1-mediated transport of atorvastatin. *Drug Metab Dispos* **38**(9)**:** 1499-1504.

Asberg A, Hartmann A, Fjeldsa E, Bergan S and Holdaas H (2001). Bilateral pharmacokinetic interaction between cyclosporine A and atorvastatin in renal transplant recipients. *Am J Transplant* **1**(4)**:** 382-386.

Backman JT, Luurila H, Neuvonen M and Neuvonen PJ (2005). Rifampin markedly decreases and gemfibrozil increases the plasma concentrations of atorvastatin and its metabolites. *Clin Pharmacol Ther* **78**(2)**:** 154-167.

Bi YA, Qiu X, Rotter CJ, Kimoto E, Piotrowski M, Varma MV, Ei-Kattan AF and Lai Y (2013). Quantitative assessment of the contribution of sodium-dependent taurocholate co-transporting polypeptide (NTCP) to the hepatic uptake of rosuvastatin, pitavastatin and fluvastatin. *Biopharm Drug Dispos*.

Choi MK, Shin HJ, Choi YL, Deng JW, Shin JG and Song IS (2011). Differential effect of genetic variants of Na(+)-taurocholate co-transporting polypeptide (NTCP) and organic anion-transporting polypeptide 1B1 (OATP1B1) on the uptake of HMG-CoA reductase inhibitors. *Xenobiotica* **41**(1)**:** 24-34.

Cui Y, Konig J, Nies AT, Pfannschmidt M, Hergt M, Franke WW, Alt W, Moll R and Keppler D (2003). Detection of the human organic anion transporters SLC21A6 (OATP2) and SLC21A8 (OATP8) in liver and hepatocellular carcinoma. *Lab Invest* **83**(4)**:** 527-538.

Elsby R, Hilgendorf C and Fenner K (2012). Understanding the critical disposition pathways of statins to assess drug-drug interaction risk during drug development: it's not just about OATP1B1. *Clin Pharmacol Ther* **92**(5)**:** 584-598.

Grube M, Kock K, Karner S, Reuther S, Ritter CA, Jedlitschky G and Kroemer HK (2006). Modification of OATP2B1-mediated transport by steroid hormones. *Mol Pharmacol* **70**(5)**:** 1735-1741.

He YJ, Zhang W, Chen Y, Guo D, Tu JH, Xu LY, Tan ZR, Chen BL, Li Z, Zhou G, Yu BN, Kirchheiner J and Zhou HH (2009). Rifampicin alters atorvastatin plasma concentration on the basis of SLCO1B1 521T>C polymorphism. *Clin Chim Acta* **405**(1-2)**:** 49-52.

Heredi-Szabo K, Jemnitz K, Kis E, Ioja E, Janossy J, Vereczkey L and Krajcsi P (2009). Potentiation of MRP2/Mrp2-mediated estradiol-17beta-glucuronide transport by drugs--a concise review. *Chem Biodivers* **6**(11)**:** 1970-1974.

Hermann M, Asberg A, Christensen H, Holdaas H, Hartmann A and Reubsaet JL (2004). Substantially elevated levels of atorvastatin and metabolites in cyclosporine-treated renal transplant recipients. *Clin Pharmacol Ther* **76**(4)**:** 388-391.

Hirano M, Maeda K, Shitara Y and Sugiyama Y (2004). Contribution of OATP2 (OATP1B1) and OATP8 (OATP1B3) to the hepatic uptake of pitavastatin in humans. *J Pharmacol Exp Ther* **311**(1)**:** 139-146.

Imanaga J, Kotegawa T, Imai H, Tsutsumi K, Yoshizato T, Ohyama T, Shirasaka Y, Tamai I, Tateishi T and Ohashi K (2011). The effects of the SLCO2B1 c.1457C > T polymorphism and apple juice

on the pharmacokinetics of fexofenadine and midazolam in humans. *Pharmacogenet Genomics* **21**(2)**:** 84-93.

Ivanov M, Kacevska M and Ingelman-Sundberg M (2012). Epigenomics and interindividual differences in drug response. *Clin Pharmacol Ther* **92**(6)**:** 727-736.

Karlgren M, Ahlin G, Bergstrom CA, Svensson R, Palm J and Artursson P (2012a). In vitro and in silico strategies to identify OATP1B1 inhibitors and predict clinical drug-drug interactions. *Pharm Res* **29**(2)**:** 411-426.

Karlgren M, Vildhede A, Norinder U, Wisniewski JR, Kimoto E, Lai Y, Haglund U and Artursson P (2012b). Classification of inhibitors of hepatic organic anion transporting polypeptides (OATPs): influence of protein expression on drug-drug interactions. *J Med Chem* **55**(10)**:** 4740-4763.

Keitel V, Burdelski M, Warskulat U, Kuhlkamp T, Keppler D, Haussinger D and Kubitz R (2005). Expression and localization of hepatobiliary transport proteins in progressive familial intrahepatic cholestasis. *Hepatology* **41**(5)**:** 1160-1172.

Kimoto E, Yoshida K, Balogh LM, Bi YA, Maeda K, El-Kattan A, Sugiyama Y and Lai Y (2012). Characterization of Organic Anion Transporting Polypeptide (OATP) Expression and Its Functional Contribution to the Uptake of Substrates in Human Hepatocytes. *Mol Pharm* **9**(12)**:** 3535–3542.

Knauer MJ, Urquhart BL, Meyer zu Schwabedissen HE, Schwarz UI, Lemke CJ, Leake BF, Kim RB and Tirona RG (2010). Human skeletal muscle drug transporters determine local exposure and toxicity of statins. *Circ Res* **106**(2)**:** 297-306.

Konig J (2011). Uptake transporters of the human OATP family: molecular characteristics, substrates, their role in drug-drug interactions, and functional consequences of polymorphisms. *Handb Exp Pharmacol*(201)**:** 1-28.

Lau YY, Huang Y, Frassetto L and Benet LZ (2007). Effect of OATP1B transporter inhibition on the pharmacokinetics of atorvastatin in healthy volunteers. *Clin Pharmacol Ther* **81**(2)**:** 194-204.

Lecluyse EL and Alexandre E (2010). Isolation and culture of primary hepatocytes from resected human liver tissue. *Methods Mol Biol* **640:** 57-82.

Lemahieu WP, Hermann M, Asberg A, Verbeke K, Holdaas H, Vanrenterghem Y and Maes BD (2005). Combined therapy with atorvastatin and calcineurin inhibitors: no interactions with tacrolimus. *Am J Transplant* **5**(9)**:** 2236-2243.

Lundquist P, Loof J, Sohlenius-Sternbeck AK, Floby E, Johansson J, Bylund J, Hoogstraate J, Afzelius L and Andersson TB (2014). The impact of solute carrier (SLC) drug uptake transporter loss in human and rat cryopreserved hepatocytes on clearance predictions. *Drug Metab Dispos* **42**(3)**:** 469-480.

Maeda K, Ikeda Y, Fujita T, Yoshida K, Azuma Y, Haruyama Y, Yamane N, Kumagai Y and Sugiyama Y (2011). Identification of the rate-determining process in the hepatic clearance of atorvastatin in a clinical cassette microdosing study. *Clin Pharmacol Ther* **90**(4)**:** 575-581.

Miyagawa M, Maeda K, Aoyama A and Sugiyama Y (2009). The eighth and ninth transmembrane domains in organic anion transporting polypeptide 1B1 affect the transport kinetics of estrone-3-sulfate and estradiol-17beta-D-glucuronide. *J Pharmacol Exp Ther* **329**(2)**:** 551-557.

Nies AT, Niemi M, Burk O, Winter S, Zanger UM, Stieger B, Schwab M and Schaeffeler E (2013). Genetics is a major determinant of expression of the human hepatic uptake transporter OATP1B1, but not of OATP1B3 and OATP2B1. *Genome Med* **5**(1)**:** 1.

Noe J, Portmann R, Brun ME and Funk C (2007). Substrate-dependent drug-drug interactions between gemfibrozil, fluvastatin and other organic anion-transporting peptide (OATP) substrates on OATP1B1, OATP2B1, and OATP1B3. *Drug Metab Dispos* **35**(8)**:** 1308-1314.

Ohtsuki S, Schaefer O, Kawakami H, Inoue T, Liehner S, Saito A, Ishiguro N, Kishimoto W, Ludwig-Schwellinger E, Ebner T and Terasaki T (2012). Simultaneous absolute protein quantification of transporters, cytochromes P450, and UDP-glucuronosyltransferases as a novel approach for the characterization of individual human liver: comparison with mRNA levels and activities. *Drug Metab Dispos* **40**(1)**:** 83-92.

Pasanen MK, Fredrikson H, Neuvonen PJ and Niemi M (2007). Different effects of SLCO1B1 polymorphism on the pharmacokinetics of atorvastatin and rosuvastatin. *Clin Pharmacol Ther* **82**(6)**:** 726-733.

Prasad B, Evers R, Gupta A, Hop CE, Salphati L, Shukla S, Ambudkar S and Unadkat JD (2013). Interindividual Variability in Hepatic Oatps and P-Glycoprotein (ABCB1) Protein Expression: Quantification by LC-MS/MS and Influence of Genotype, Age and Sex. *Drug Metab Dispos*.

Qiu X, Bi YA, Balogh LM and Lai Y (2013). Absolute measurement of species differences in sodium taurocholate cotransporting polypeptide (NTCP/Ntcp) and its modulation in cultured hepatocytes. *J Pharm Sci*.

Roma MG, Crocenzi FA and Mottino AD (2008). Dynamic localization of hepatocellular transporters in health and disease. *World J Gastroenterol* **14**(44)**:** 6786-6801.

Shitara Y, Maeda K, Ikejiri K, Yoshida K, Horie T and Sugiyama Y (2013). Clinical significance of organic anion transporting polypeptides (OATPs) in drug disposition: their roles in hepatic clearance and intestinal absorption. *Biopharm Drug Dispos* **34**(1)**:** 45-78.

Soars MG, Barton P, Ismair M, Jupp R and Riley RJ (2012). The Development, Characterization, and Application of an OATP1B1 Inhibition Assay in Drug Discovery. *Drug Metab Dispos* **40**(8)**:** 1641-1648.

Watanabe T, Kusuhara H, Maeda K, Kanamaru H, Saito Y, Hu Z and Sugiyama Y (2010). Investigation of the rate-determining process in the hepatic elimination of HMG-CoA reductase inhibitors in rats and humans. *Drug Metab Dispos* **38**(2)**:** 215-222.

Wen X, Wang JS, Backman JT, Kivisto KT and Neuvonen PJ (2001). Gemfibrozil is a potent inhibitor of human cytochrome P450 2C9. *Drug Metab Dispos* **29**(11)**:** 1359-1361.

Whitfield LR, Porcari AR, Alvey C, Abel R, Bullen W and Hartman D (2011). Effect of gemfibrozil and fenofibrate on the pharmacokinetics of atorvastatin. *J Clin Pharmacol* **51**(3)**:** 378-388.

Wisniewski JR, Ostasiewicz P, Dus K, Zielinska DF, Gnad F and Mann M (2012). Extensive quantitative remodeling of the proteome between normal colon tissue and adenocarcinoma. *Mol Syst Biol* **8:** 611.

Wisniewski JR, Zougman A, Nagaraj N and Mann M (2009). Universal sample preparation method for proteome analysis. *Nat Methods* **6**(5)**:** 359-362.

DMD Fast Forward. Published on May 5, 2014 as DOI: 10.1124/dmd.113.056309

Yoshida K, Maeda K and Sugiyama Y (2012). Transporter-mediated drug--drug interactions involving OATP substrates: predictions based on in vitro inhibition studies. *Clin Pharmacol Ther* **91**(6)**:** 1053-1064.

Footnotes

This work was supported by the Swedish Research Council [grant approval no. 2822]; the Swedish Fund for Research without Animal Experiments; the Lars Hierta Memorial Foundation; and O.E. and Edla Johansson's Scientific Foundation.

Part of this work was presented at the joint 19th MDO and 12th European ISSX Meeting 2012.

Person to receive reprint requests:

Per Artursson, PhD, Professor in Dosage Form Design

Department of Pharmacy, Uppsala University, Box 580, SE-751 23 Uppsala, Sweden

Email: per.artursson@farmaci.uu.se

Present address of Y.L: Pharmaceutical Candidate Optimization, Bristol-Myers Squibb, Princeton, New Jersey, USA.

Legends for Figures

Figure 1. Atorvastatin uptake in NTCP-HEK293 cells. (A) Uptake of atorvastatin in cells expressing NTCP compared to passive uptake in mock-transfected cells. Data represent the mean and standard deviation of 12 independent experiments, each run in triplicate. (B) Kinetic profile of NTCP-mediated uptake of atorvastatin and passive diffusion in mock-transfected cells. Atorvastatin uptake in HEK293 cells either stably transfected with NTCP or mock-transfected was measured over a range of ten concentrations between 0.1 and 800 µM. Data represent the uptake rate measured in duplicate in one representative experiment.

Figure 2. Label-free protein quantification of uptake transporters in human liver tissue. Protein expression levels of OATP1B1 (A), OATP1B3 (B), OATP2B1 (C), and NTCP (D) in crude membrane fractions from twelve human livers. Protein abundance were calculated from the ratio of the summed signal intensities of the peptides identifying each protein to the signal intensities of all peptides identified for the human liver proteome (> 4000 proteins). The last bar represents the arithmetic mean expression for the twelve samples with standard deviation.

Figure 3. Atorvastatin hepatic uptake. Prediction of *in vivo* intrinsic hepatic uptake clearance (CL int,uptake) of atorvastatin based on protein expression data in human liver and *in vitro* cell models. The dotted line represents the mean intrinsic uptake CL for the twelve livers. The hepatic clearance via passive diffusion (CLpassive) was predicted to be the same as that observed in HEK293 cells (120 µL min^{-1} g $liver^{-1}$). OATP1B1 and OATP1B3 were predicted to contribute to the majority of the hepatic atorvastatin uptake.

Figure 4. Atorvastatin and taurocholate uptake in human hepatocytes in sodium-containing (control) and sodium-free buffer after 2 min incubation with a concentration of 1 µM. Data

shown as mean ± S.D (n=4) from a representative experiment. *** P<0.001 compared with control.

Figure 5. Inhibition of OATP1B1-, OATP1B3-, OATP2B1- and NTCP-mediated uptake of atorvastatin by atazanavir (A), cyclosporine (B), gemfibrozil (C), lopinavir (D), and rifampicin (E) in stably transfected HEK293 cells. The cells were incubated with 1 µM atorvastatin and increasing concentrations of the potential inhibitors for 2 min at 37 °C. Data represent mean ± S.E.M.

Figure 6. Impact of drug-drug interactions on predicted atorvastatin uptake clearance. Remaining intrinsic uptake clearance upon co-administration of five different inhibitors is shown for the twelve livers. Co-administration of gemfibrozil was predicted to have a minor impact on atorvastatin uptake CL, while co-administration of atazanavir, cyclosporine, lopinavir, and rifampicin was predicted to give a more pronounced reduction in atorvastatin uptake.

Figure 7. Inhibition of atorvastatin uptake by atazanavir, cyclosporine, gemfibrozil, lopinavir and rifampicin in human hepatocytes. Atorvastatin (1 µM) was incubated in the presence and absence of the potential inhibitors. Uptake clearance was determined from the slope of the curves. Data shown as mean ± S.D (n=3) from a representative experiment.

Tables

Table 1. Kinetic parameters of NTCP-, OATP1B1-, OATP1B3-, and OATP2B1-mediated atorvastatin uptake in stably transfected HEK293 cells.

Transporter	K_m (μM)	V_{max} (pmol min^{-1} mg $protein^{-1}$)
NTCP	185 ± 108	2260 ± 1184
OATP1B1	0.77 ± 0.24[a]	6.61 ± 1.24[a]
OATP1B3	0.73 ± 1.45[a]	10.12 ± 1.78[a]
OATP2B1	2.84 ± 1.63[a]	455.2 ± 55.36[a]

[a] K_m and V_{max} values reprinted with permission from (Karlgren *et al.*, 2012b). Copyright (2012) American Chemical Society.

DMD Fast Forward. Published on May 5, 2014 as DOI: 10.1124/dmd.113.056309

Table 2. Protein expression levels of uptake transporters in human liver membrane fractions.

Transporter	*n*	Protein expression level (fmol μg membrane protein^{-1})				
		Mean ± S.D	Median	Min	Max	Max/Min
NTCP	12	1.8 ± 0.5	1.2	0.5	3.9	7.5
OATP1B1	12	23.2 ± 9.4	19.6	12.1	44.4	3.7
OATP1B3	12	3.2 ± 0.2	3.8	0.2	6.0	32.0
OATP2B1	12	1.6 ± 0.6	1.5	0.6	4.3	7.5

Max, maximum; Min, minimum; Max/Min, fold range in expression

DMD Fast Forward. Published on May 5, 2014 as DOI: 10.1124/dmd.113.056309

Table 3. Half-maximal inhibitory concentrations, IC_{50}, and corresponding inhibition constants, K_i, calculated assuming competitive inhibition.

	OATP1B1		**OATP1B3**		**OATP2B1**		**NTCP**	
	IC_{50} (μM)	K_i (μM)	IC_{50} (μM)	K_i (μM)	IC_{50} (μM)	K_i (μM)	IC_{50} (μM)	K_i (μM)
Atazanavir	0.96	0.42	17	7.3	>40	>30	>40	>40
Cyclosporine	1.5	0.66	3.1	1.3	>18	>13	4.8	4.8
Gemfibrozil	130	58	>1000	>420	770	570	89	89
Lopinavir	0.77	0.34	>10	>4.2	>10	>7.4	>10	>10
Rifampicin	5.0	2.2	190	82	>630	>470	>630	>630

DMD Fast Forward. Published on May 5, 2014 as DOI: 10.1124/dmd.113.056309

Table 4. Comparison of half-maximal inhibitory concentrations, IC_{50}, determined *in vitro* using either atorvastatin or an endogenous substrate.

	OATP1B1		**OATP1B3**		**OATP2B1**	
	IC_{50} (μM) Atorvastatin	IC_{50} (μM) E17βG[a]	IC_{50} (μM) Atorvastatin	IC_{50} (μM) E17βG[a]	IC_{50} (μM) Atorvastatin	IC_{50} (μM) E3S[a]
Atazanavir	0.96 ± 1.2	1.4 ± 1.0	17 ± 1.3	0.40 ± 1.2	>40	5.2 ± 1.2
Cyclosporine	1.5 ± 1.2	1.4 ± 1.2	3.1 ± 1.4	1.3 ± 1.0	>18	37 ± 1.6
Rifampicin	5.0 ± 1.2	1.2 ± 1.2	190 ± 1.7	1.5 ± 1.1	>630	65 ± 1.2

E17βG, estradiol-17β-glucuronide; E3S, estrone-3-sulphate

[a] IC_{50}-values reprinted with permission from (Karlgren *et al.*, 2012b). Copyright (2012) American Chemical Society.

DMD Fast Forward. Published on May 5, 2014 as DOI: 10.1124/dmd.113.056309

Figure 1

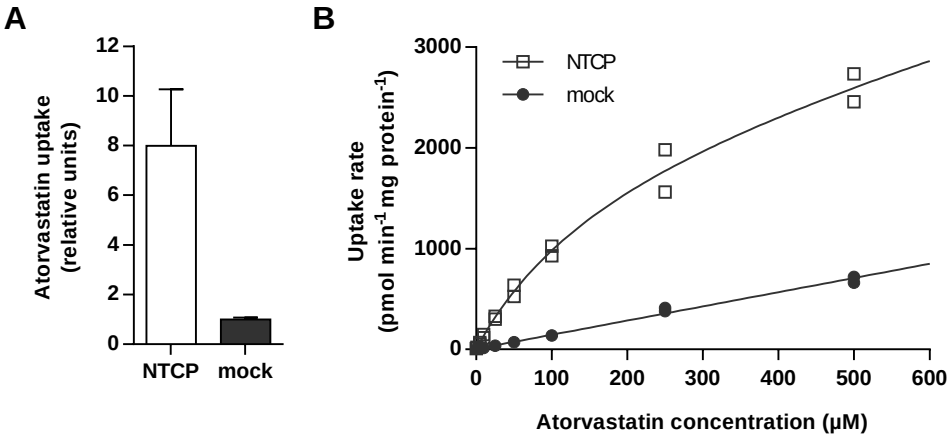

DMD Fast Forward. Published on May 5, 2014 as DOI: 10.1124/dmd.113.056309

Figure 2

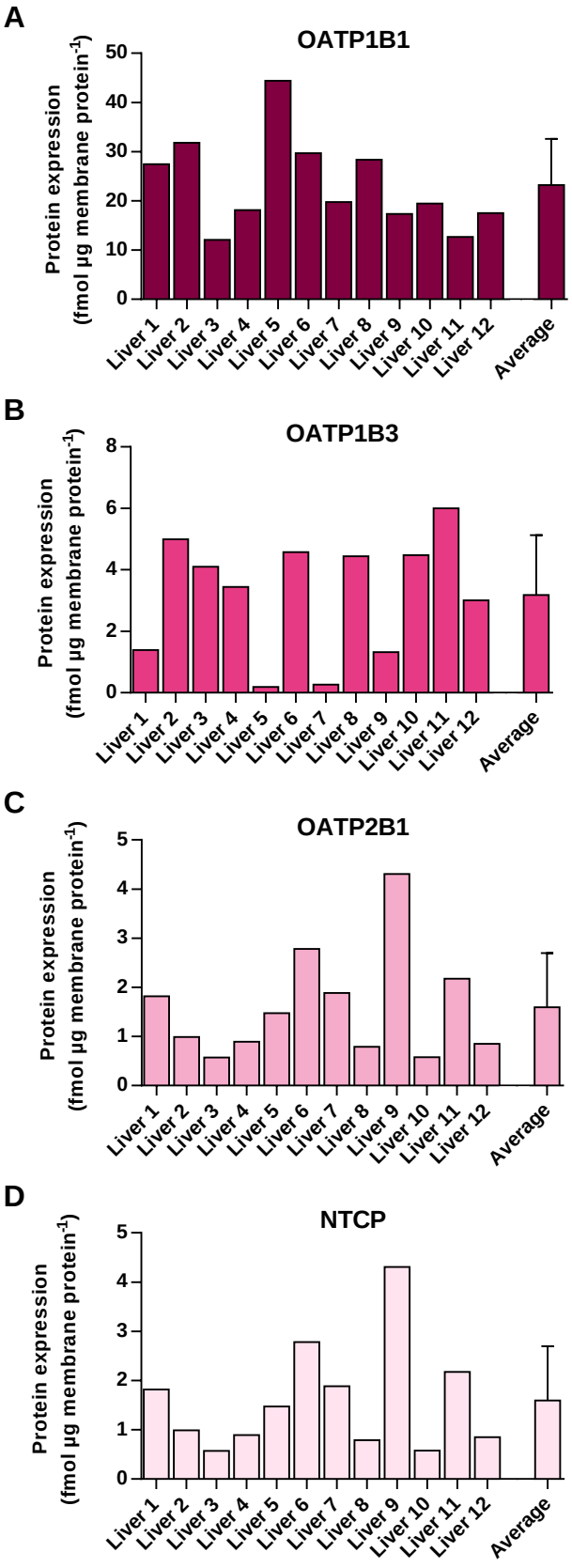

Figure 3

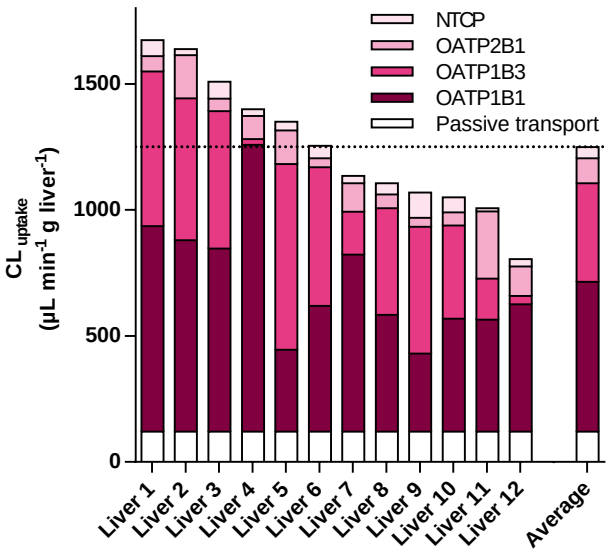

Figure 4

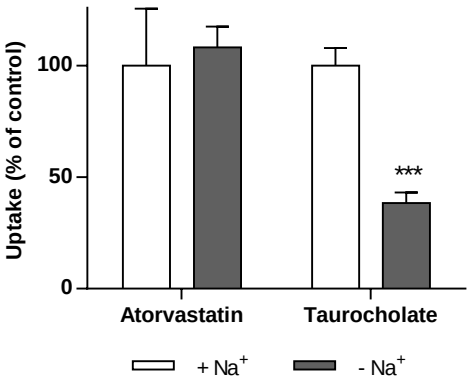

DMD Fast Forward. Published on May 5, 2014 as DOI: 10.1124/dmd.113.056309

Figure 5

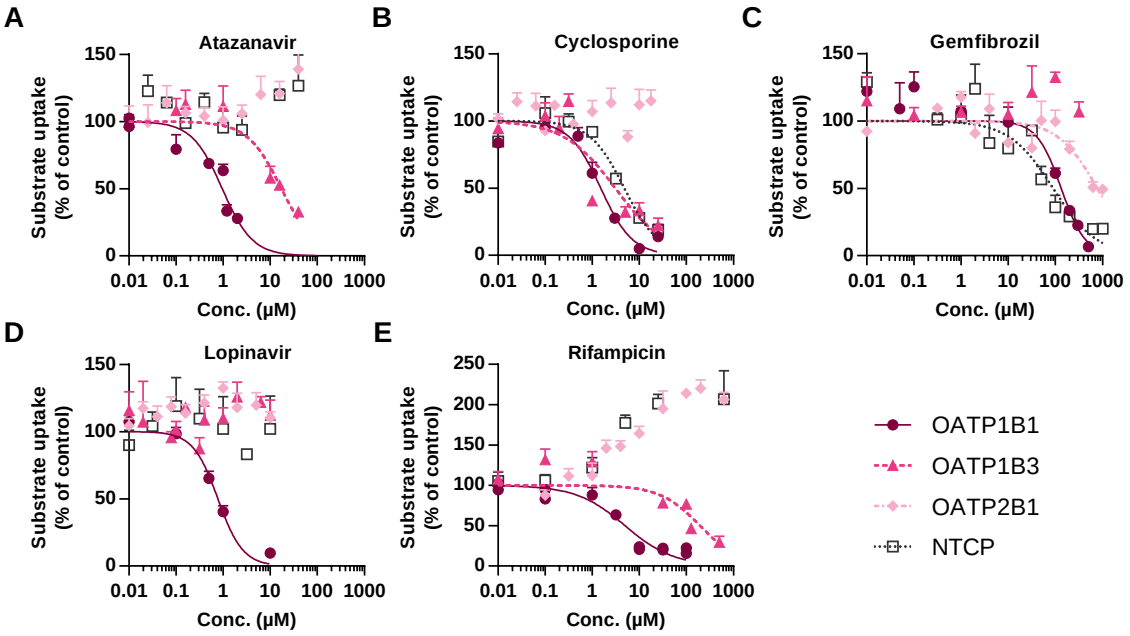

Figure 6

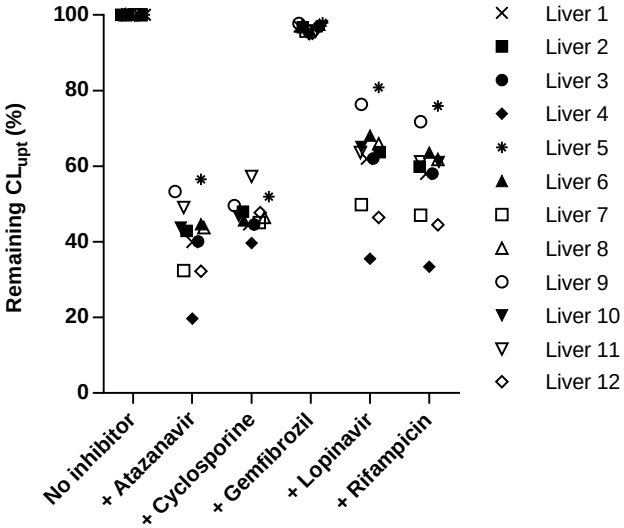

DMD Fast Forward. Published on May 5, 2014 as DOI: 10.1124/dmd.113.056309

Figure 7